Journal of Applied Polymer Science

Morphology and crystallization behavior of PCL/SAN blends containing nanosilica with different surface properties

Jing Qian, Zhilin Xiao, Lin Dong, Dahang Tang, Mengjue Li, Qi Yang, Yajiang Huang, Xia Liao
State Key Laboratory of Polymer Materials Engineering of China, College of Polymer Science and Engineering, Sichuan University, Chengdu 610065, China
Correspondence to: Q. Yang (E-mail: yangqi@scu.edu.cn)

ABSTRACT: Morphology and crystallization behavior of poly(ε-caprolactone) (PCL) in its 80/20 blends with poly(styrene-co-acrylonitrile) (SAN) containing hydrophobic or hydrophilic nanosilica was investigated. It was found that hydrophilic nanosilica displayed a more significant refinement effect on co-continuous morphology of PCL/SAN blends than hydrophobic nanosilica for its selective distribution within the PCL matrix but closer to the two-phase interface. Ring-banded spherulites were observed in both kinds of nanosilica-filled blends, the periodic distance of which decreased with increasing nanosilica content. Hydrophilic nanosilica reduced the dependence of the periodic distance of ring-banded spherulites on the crystallization temperature more efficiently than hydrophobic nanosilica. Furthermore, crystallization process of PCL/SAN blends filled with hydrophobic nanosilica was suppressed as the restriction effect of nanosilica on the crystal growth always outweighed their heterogeneous nucleation effect. In contrast, low content of hydrophilic nanosilica ($\leq$1 wt %) were more likely to exhibit growth restriction effect rather than nucleation effect, whereas heterogeneous nucleation effect of higher content of hydrophilic nanosilica (>1 wt %) dominated over growth restriction effect on facilitating the crystallization behavior. © 2016 Wiley Periodicals, Inc. J. Appl. Polym. Sci. **2016**, *133*, 44157.

KEYWORDS: blends; crystallization; morphology; nanoparticles; nanowires and nanocrystals

Received 8 May 2016; accepted 3 July 2016
DOI: 10.1002/app.44157

INTRODUCTION

Poly(ε-caprolactone) (PCL) in blends with poly(styrene-co-acrylonitrile) (SAN) containing 8 to 28 wt % acrylonitrile (AN) is miscible. If AN content is less than 6 wt % or greater than 30 wt %, the blends become immiscible.[1] Besides the miscibility studies, crystallization behavior and morphology investigations on PCL/SAN blends have also been attracting considerable attention. Crystallization leads to ring-banded spherulites in miscible PCL/SAN blends while immiscible PCL/SAN blends exhibit only common spherulitic structure.[2] Periodic distance of ring-banded spherulites is generally used as parameters to quantify the effect of amorphous component on the twisting of PCL lamellar, which is accorded with the compatibility of the blends.[3,4] In the crystalline (PCL) and noncrystalline (SAN) blends, the factors such as the chain mobility, nucleation free energy, and competition between the advancing spherulitic front of a crystallizable polymer (PCL) and diffusion of an amorphous polymer (SAN) into interlamellar regions can be summarized to influence spherulites growth kinetics.[5,6] Kresller *et al.*[7] found the minimum radial spherulites growth rate of PCL/SAN blends when SAN contains 20 wt % AN. Chiu *et al.*[1] reported that the glass transition temperature (T_g) of PCL/SAN blends significantly increased with SAN content increasing, implying more restriction effect on the crystallization kinetics. Actually, PCL/SAN blends were typically chosen mainly because of the suitable spherulites growth rate under controlled conditions and the ability to form regular bands in a fairly wide crystallization temperature range.

Nanofillers have attracted a rising interest in previous studies as they can not only play a critical role in determining the crystallization behavior of blends but also control the morphology of polymer blends.[8–14] That can be attributed to the following aspects. On one hand, nanofillers have excellent advantage as nucleating agent. Mdletshe *et al.*[12] found that adding silicon carbide nanoparticles into PCL would increase cooling crystallization temperature (T_c), implying that nanoparticles have nucleating effects. Nanoparticles have also been proven efficient heterogeneous nucleating agents in PP/PS blends and PP/PET blends.[10,14] On the other hand, the introduction of nanoparticles into blends as compatibilizers to control the morphology structure of blends has also been widely reported. Laoutid *et al.*[9] had shown that the nanosilica strongly reduced the droplet size of disperse phase. Because nanosilica tended to place preferentially at the interface of PP/PC blends, which could alter

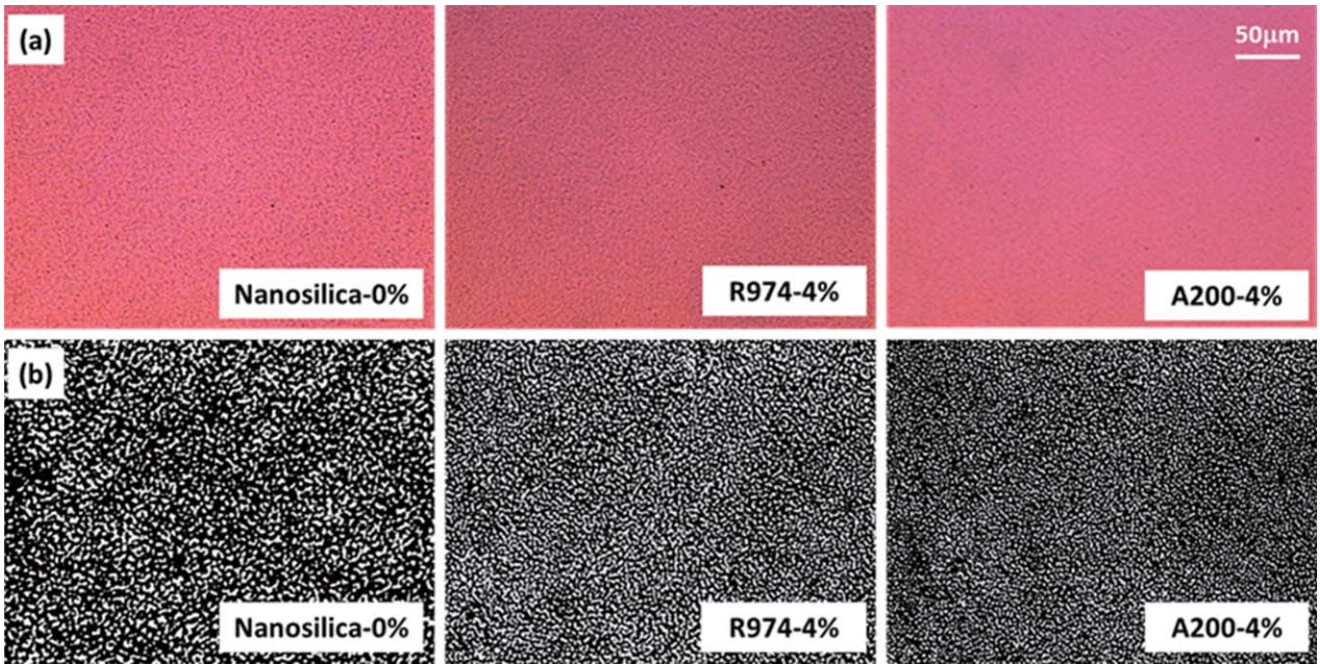

Figure 1. The phase morphology of (a) PCL/SAN-30/Nanosilica (80/20/*x*) at 100 °C, and (b) are binary images processed by the software Imlviewer. [Color figure can be viewed in the online issue, which is available at wileyonlinelibrary.com.]

the interfacial tension and keep the droplets from coalescing. Martin *et al.*[8] studied the influence of nanosilica with different surface chemistries on the co-continuous morphology of PP/EPDM blends. It suggested that the hydrophilic nanosilica dispersed within the EPDM phase hardly perturbed the morphology while hydrophobic nanosilica located both within the EPDM phase and at the interface had a better physical compatibilization, which would decrease viscosity ratio, leading to a very similar co-continuous morphology.

To our best knowledge, most studies for blends exhibiting ring-banded spherulites have been carried out, which focus on the effect of blending proportion, crystallization temperature, or molecular weight on the morphology and crystallization behavior. However, in nanofiller-filled blends with crystallizable rich phase, the morphology and crystallization changes may be caused by the heterogeneous nucleation effect and the morphological refinement effect of nanofillers simultaneously, which were studied in limited papers. In addition, although it has been confirmed that AN content, temperature and blend ratio will alter the ring-banded morphology and crystallization behavior noticeably in PCL/SAN blends, the nanosilica as third component filled in the blends has not been investigated systematically yet. Furthermore, the aforementioned researches indicate that the distribution of nanosilica is of great importance to morphology and crystallization behavior in polymer composites. Thus, the incorporation of nanosilica with different surface properties (hydrophilic or hydrophobic) in PCL/SAN blends would lead to innovative and interesting results.

Hence, PCL/SAN-30 (code: SAN-*x*, x = wt % of AN) blends with nanosilica concentration ranging from 0 to 4 wt % were prepared by continuous mechanical mixing in 1,2-dichloroethane. We found significant reductions in characteristic size of co-continuous morphology as nanosilica were introduced. The ring-banded spherulites were observed in PCL/SAN-30 blends with or without nanosilica. Thermodynamic analysis was performed to explore the effect of concentration and surface properties of nanosilica on the morphology of the composites. In addition, the crystallization behavior was analyzed from two aspects, including the spherulite growth restriction effect and the heterogeneous nucleation effect induced by nanosilica.

EXPERIMENTAL

Materials

PCL and SAN with 30 wt % AN content are supplied by Aldrich. Their weight average of molecular weight (M_w) are 1.4 $\times$ 10^4 g/mol^{-1} and 1.85 $\times$ 10^5 g/mol^{-1}, respectively. 1, 2-dichloroethane is supplied by Crowncolor. The M_w is 98.95. Hydrophobic nanosilica (Aerosil R974) with specific surface area of 170 $\pm$ 20 m^2/g and hydrophilic nanosilica (Aerosil A200) with specific surface area of 200 $\pm$ 25 m^2/g filled in PCL/SAN-30 blends are provided by Degussa Corp. Their diameters are both 12 nm.

Sample Preparation

All blends were prepared by continuous mechanical mixing in 1, 2-dichloroethane. The concentration of the polymer solution was 3 wt %. The composition between PCL/SAN was 80/20. The weight fraction of nanosilica was 0, 0.5, 1, 2, 4 wt % of the total weight of the blends. To achieve a good dispersion state of nanosilica in the blends, all the solutions were oscillated with an ultrasonicator (BILON98-IIIDL from Shanghai Bilon Instruments, LTD) at a power of 500 W for 30 min. After that, the polymer solutions were casted onto cover glass and polytetrafluoroethene (PTFE) plates, and then placed in fuming hood at room temperature for a week. After another vacuum drying at

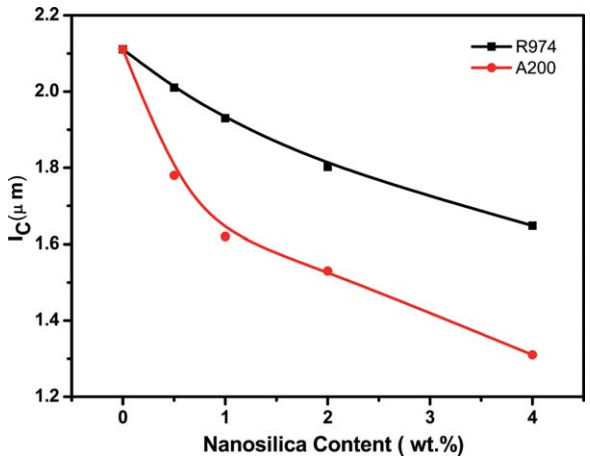

Figure 2. The characteristic size of co-continuous morphology with the increasing nanosilica content. [Color figure can be viewed in the online issue, which is available at wileyonlinelibrary.com.]

40 °C for 48 h, film with the thickness about 10 μm on cover glass and about 100 μm on PTFE plates were obtained.

Characterization

Polarized optical microscope (POM) (Olympus; Tokyo, Japan) equipped with a Pixel INK CCD camera and a hot stage (Linkam LTS350, UK) was used to observe morphology and crystallization process. Each sample annealed at 100 °C for 5 min to eliminate thermal history. Following this, they were quickly cooled to the designated temperature for isothermal crystallization. The ring-banded structure was further identified by scanning electron microscopy (SEM; JEOLSJM-5900VL) operating at 20 kV. The samples for SEM testing were obtained after completely isothermal crystallization and coated with a thin gold layer. The distribution of nanosilica in PCL/SAN-30 blends was characterized by a transmission electron microscope (Tecnai, G2 F20) at an acceleration voltage of 200 kV. OsO4 vapor was performed to stain the ultrathin sections of about 50 nm thick for 1 h. The periodic distance of rings and characteristic size were analyzed using the software Imlviewer and LineLength (programmed by our laboratory team).

Dynamic rheological measurements were performed on an advanced rheumatic expansion system analyzer (ARES, TA Instruments, USA) equipped with parallel plates of 25 mm in diameter. The chosen gap was 0.8 mm for all measurements. The test temperature was maintained at 100 °C ensuring all blends remained in melted state. The frequency range was from 0.1 to 100 rad/s, holding 5% strain value in the linear viscoelastic region.

Table I. Surface Tension Data of the Components of the Blends at 25 °C[10,24]

	Surface tension (mN/m)			γ(0) (mN/m)	T_{cr} (K)	$d\gamma/dT$ [(mN/m)/K]
	γ	γ^d	γ^p			
PCL	52.3	42.1	10.2	73.7	1220	—
SAN	38.5	30.61	7.89	50.5	1499	—
R974	81.7	72.3	9.4	—	—	−0.1
A200	80	29.4	50.6	—	—	−0.1

Differential scanning calorimeter (DSC Q20, TA Instruments) was used to characterize crystallization behavior. Two kinds of DSC measurements were performed: (i) The samples were first hold in 40 °C for 0.5 min, then heated quickly to 100 °C and annealed for 3 min to eliminate the thermal history. After that, the samples were cooled down to −20 °C and then heated to 150 °C again at a rate of 10 °C/min; and (ii) The samples were first held in 40 °C for 0.5 min, then heated quickly to 100 °C and annealed for 3 min to eliminate the thermal history. After that, the samples were cooled down to designated temperature, and held for enough time for isothermal crystallization.

DMA measurements (DMA Q800, TA Instruments, USA) were performed at a heating rate of 3 K/min and 1 Hz in nitrogen atmosphere to evaluate the T_g of the polymer blends. The temperature corresponding to the maximal loss moduli "G" was regarded as T_g for the blends.[15]

RESULTS AND DISCUSSION

Phase Morphology of PCL/SAN/Nanosilica Blends

The discrepant morphology of PCL/SAN-30(80/20) blends filled with nanosilica at 100 °C are shown in Figure 1(a,b). There is an appearance of co-continuous morphology in all blends with or without nanosilica, implying that the critical blends go through a phase separation at 100 °C, finally manifesting spinodal decomposition structure. And the characteristic size of co-

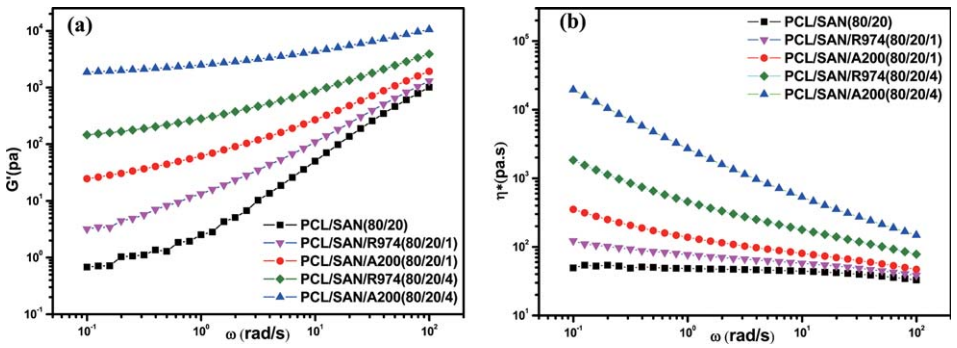

Figure 3. Dependence of (a) storage modulus, G', and (b) complex viscosity, η*, on frequency for the PCL/SAN-30 (80/20) blends in the presence of different contents of nanosilica. [Color figure can be viewed in the online issue, which is available at wileyonlinelibrary.com.]

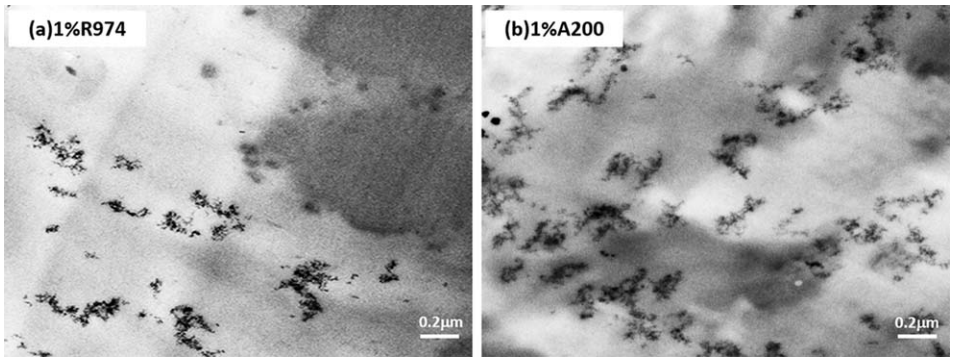

Figure 4. TEM image showing the location of nanosilica in PCL/SAN-30 (80/20) blends. The light gray domain is the PCL phase. The dark gray domain is the stained SAN phase. The darkest dots are the nanosilica.

continuous morphology [the average value of the white and black size in Figure 1(b)] is found to diminish with the increase of nanosilica content. Figure 2 reveals the detailed change of the characteristic size of co-continuous structure, which decreases with increasing nanosilica content for both R974 and A200 filled PCL/SAN-30 blends. The decrease trend, however, is more evident for PCL/SAN-30/A200 blends. Lee *et al.*[16] also found nanosilica could reduce the coalescence rate of the dispersed phase domains, generating a better dispersed domains and a finer co-continuous morphology in Poly(propylene)/Ethylene-Octene copolymer blends. These results indicate nanosilica, as compatibilizer, display a morphological refinement effect, but finer morphology with smaller characteristic size of the PCL/SAN-30/A200 blends suggests that the hydrophilic nanosilica make a more significant compatibilization.

To further verify above conclusion, additional evidence is provided by dynamic rheological measurements, which is an effective method to demonstrate melted structures such as the distribution state of nanoparticles and the phase morphology.[17,18] Figure 3 shows the storage modulus and complex viscosity of pure PCL/SAN-30 and nanosilica filled PCL/SAN-30 blends as a function of frequency at 100 °C. The viscosity of pure PCL/SAN-30 blends is very low and independent of frequency in the restrained frequency range, as shown in Figure 3(b). As the content of nanosilica increases, both G' and η^* of composites increase, indicating that nanosilica greatly change the viscoelasticity of composites. Furthermore, there is a tendency that the G' of PCL/SAN-30/Nanosilica blends become independent on frequency, meanwhile the viscosity strongly rise in the low frequency region. This may expose the formation of a three dimensional physical network.[19] Gubbels *et al.*[17] elaborated the relationship between the development mechanism of a particle network and the concentration of nanoparticles, which may be applied to the situation of high content of hydrophilic nanosilica. Accordingly, the viscosity variations of these blends with nanosilica are different. At lowest frequency region, the η^* of PCL/SAN-30/A200 (80/20/4) is nearly 400 times of pure PCL/SAN-30 blends, while $\eta^*$of blends with 4 wt % R974 is only 40 times. Same phenomenon related with the concentration and surface chemistries of nanoparticles have also been found in PS/PVME/Nanosilica blends and many other nanoparticle filled composites.[20] The higher viscosity of PCL/SAN-30/A200 blends can be attributed to the enhanced compatibilization of A200 and more areas of phase interface [see Figure 1(a,b)], compared to PCL/SAN-30/R974 blends.

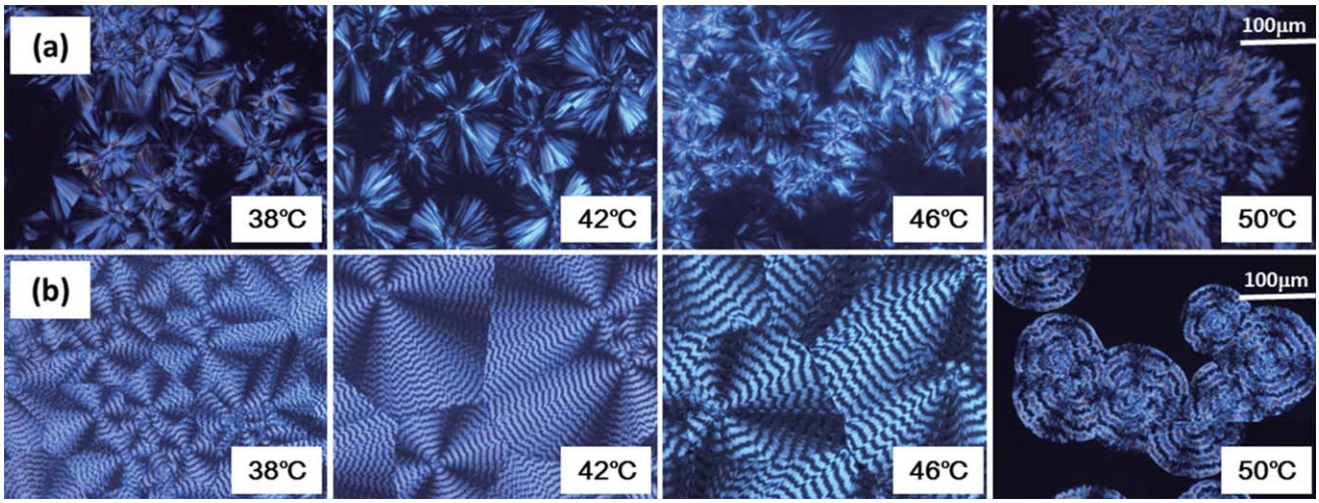

Figure 5. POM micrographs for (a) pure PCL, and (b) PCL/SAN-30 (80/20) blends, crystallized at different temperatures. [Color figure can be viewed in the online issue, which is available at wileyonlinelibrary.com.]

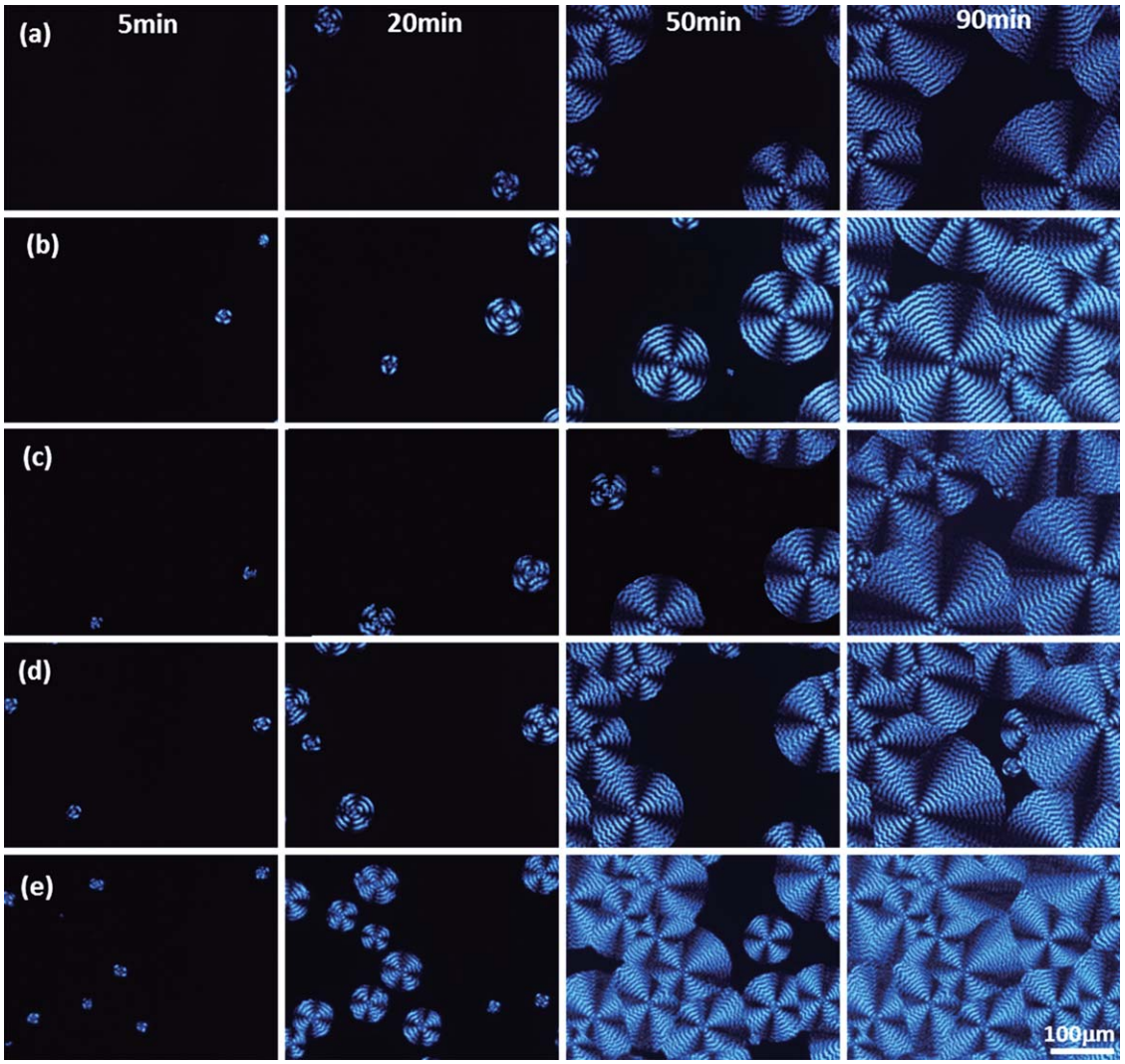

Figure 6. Morphology evolution of PCL/SAN-30 (80/20) blends with varying R974 contents: (a) 0 wt %; (b) 0.5 wt %; (c) 1 wt %; (d0 2 wt %; (e) 4 wt % crystallized at 42 °C. [Color figure can be viewed in the online issue, which is available at wileyonlinelibrary.com.]

The localization of nanosilica in PCL/SAN-30 blends can be predicted qualitatively using a wetting parameter ω,[21]

$$\omega_1 = \frac{\gamma_{si-2} - \gamma_{si-1}}{\gamma_{12}} \quad (1)$$

where γ_{si-i} is the interfacial tension between the polymer i and the nanosilica and γ_{12} is the interfacial tension between the two components. When $\omega_1 > 1$, the nanosilica particles are located only in polymer 1. When $\omega_1 < -1$, the nanosilica particles are only present in polymer 2. When $-1 < \omega_1 < 1$, the nanosilica particles are located at the interface between two polymers. The interfacial tension between two components can be estimated by the Owens and Wendt equation,[22]

$$\gamma_{12} = \gamma_1 + \gamma_2 - 2\sqrt{\gamma_1^d \gamma_2^d} - 2\sqrt{\gamma_1^p \gamma_2^p} \quad (2)$$

where the superscript d and p stand for the dispersive and the polar contributions to the surface tension, respectively. The surface tension of polymeric component at 100 °C can be estimated from the relationship proposed by Guggenheim,[23]

$$\gamma = \gamma(0) * (1 - T/T_{cr})^{11/9} \quad (3)$$

where the $\gamma(0)$ is surface tension at 25 °C and T_{cr} is the experimental value of critical temperature. The values of γ^d, γ^P, $\gamma(0)$, and T_{cr} of polymeric components and nanosilica are given in Table I. Assuming that the temperature dependence of each contribution follows the same law as for the surface tension, then it can use eq. (3) to estimate γ^d and γ^P at 100 °C. For nanosilica, the surface tension is estimated at 100 °C using the rate $d\gamma/dT$ which is assumed to be constant in the interval of temperature used.[25]

For PCL/SAN-30 blends at 100 °C, it is found that ω is 8.95 for R974 and 1.30 for A200. Thus, R974 should be preferentially located within PCL phase. And A200 mainly distribute alongside the interface of PCL phase and SAN phase. Note that the blending conditions will also influence the distribution of nanosilica, so it is further verified by the TEM images [Figure 4(a,b)]. Owing to the selective distribution in the PCL component in the blends, both types of nanosilica can compensate the

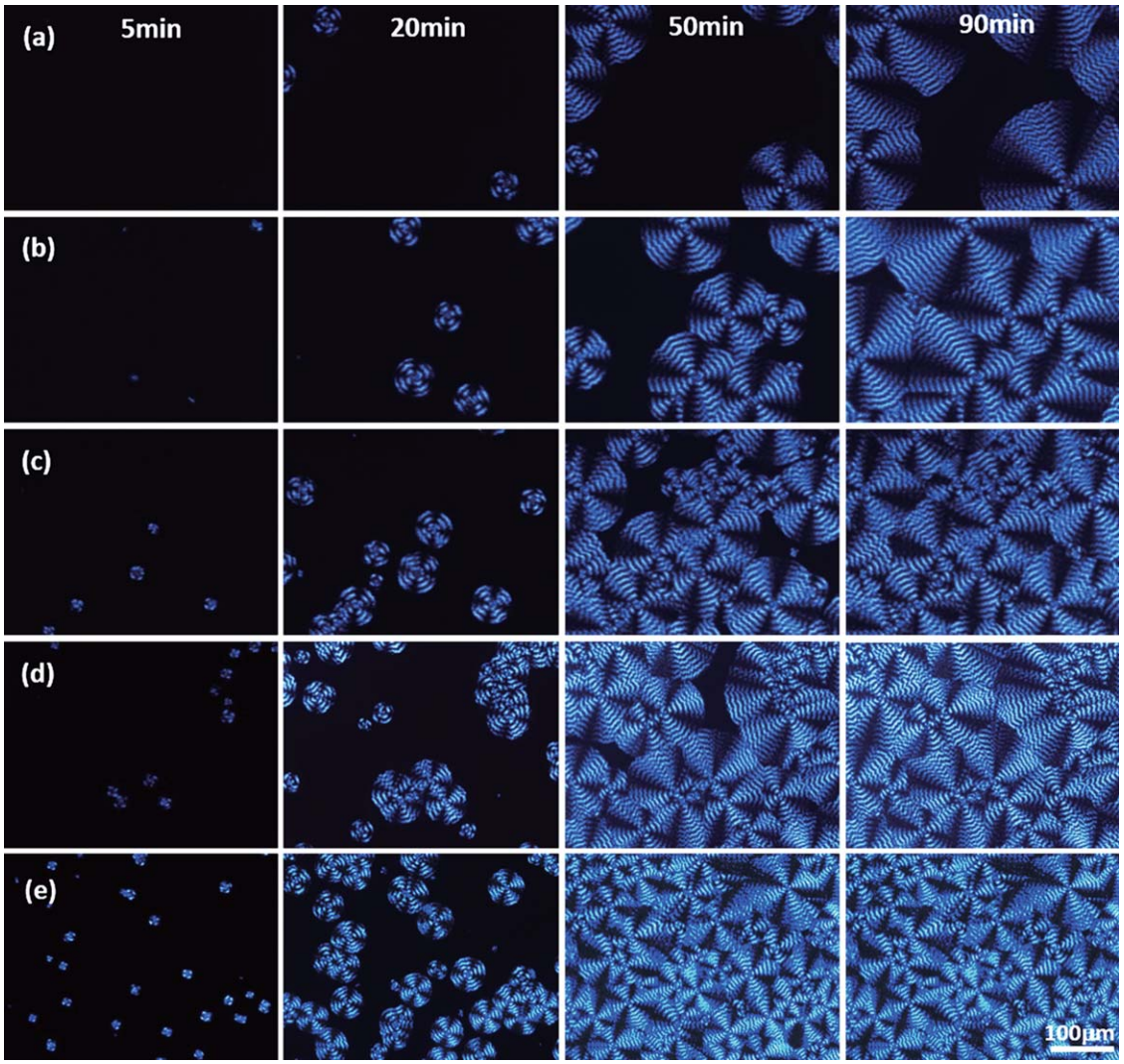

Figure 7. Morphology evolution of PCL/SAN-30 (80/20) blends with varying A200 contents: (a) 0 wt %; (b) 0.5 wt %; (c) 1 wt %; (d) 2 wt %; (e) 4 wt % crystallized at 42 °C. [Color figure can be viewed in the online issue, which is available at wileyonlinelibrary.com.]

increase of viscosity ratio and change the phase morphology. Matching the work of Elias's,[25] nanosilica locating in one phase of the co-continuous structure exist a physical compatibilization, which will reduce the viscosity ratio and suppress the coarsening process. In addition, the inhomogeneous distribution of A200 alongside the interface efficiently inhibits the dispersed phase gathering on the kinetics.[25,26]

Based on the discussions above, it can be concluded that the incorporation of hydrophilic nanosilica in PCL/SAN-30 blends lead to a higher degree of compatibilization than hydrophobic nanosilica, accompanying with tinier co-continuous morphology.

Isothermal Crystallization Morphology of PCL/SAN/Nanosilica Blends

Figure 5 shows the POM micrographs of pure PCL and PCL/SAN-30 blends crystallized at different temperatures. The pure PCL melt exhibits only common spherulites with Maltese-cross while typical ring-banded spherulites are observed in the PCL/SAN-30 blends although the temperature is lower than 50 °C. Apparently, the less decomposed blends redissolve rapidly before the crystallization take place, or the blends would develop the regular spherulites as pure PCL (i.e., no ring-banded structure).[27–29] In addition, there is a temperature limit to observe the ring-banded pattern. When crystallization temperature is close to melting temperature, crystallization process become quite slowly, thus the online observation and dynamics statistic are made fairly difficult. When crystallization temperature is relatively low, the number of ring-banded spherulites increases but their diameters decline. Hence, it can hardly be observed several rings within single spherulites. Preliminary experiments are implemented to find the most suitable temperature of 42 °C to research the crystallization behavior.[28]

The isothermal crystalline morphology evolution of PCL/SAN-30/Nanosilica blends, with nanosilica concentration ranging from 0 to 4 wt % are investigated, as shown in Figures 6 and 7. For PCL/SAN-30 blends with or without R974, shown in Figure 6(a–e), a distinct ring-banded pattern can be observed. The

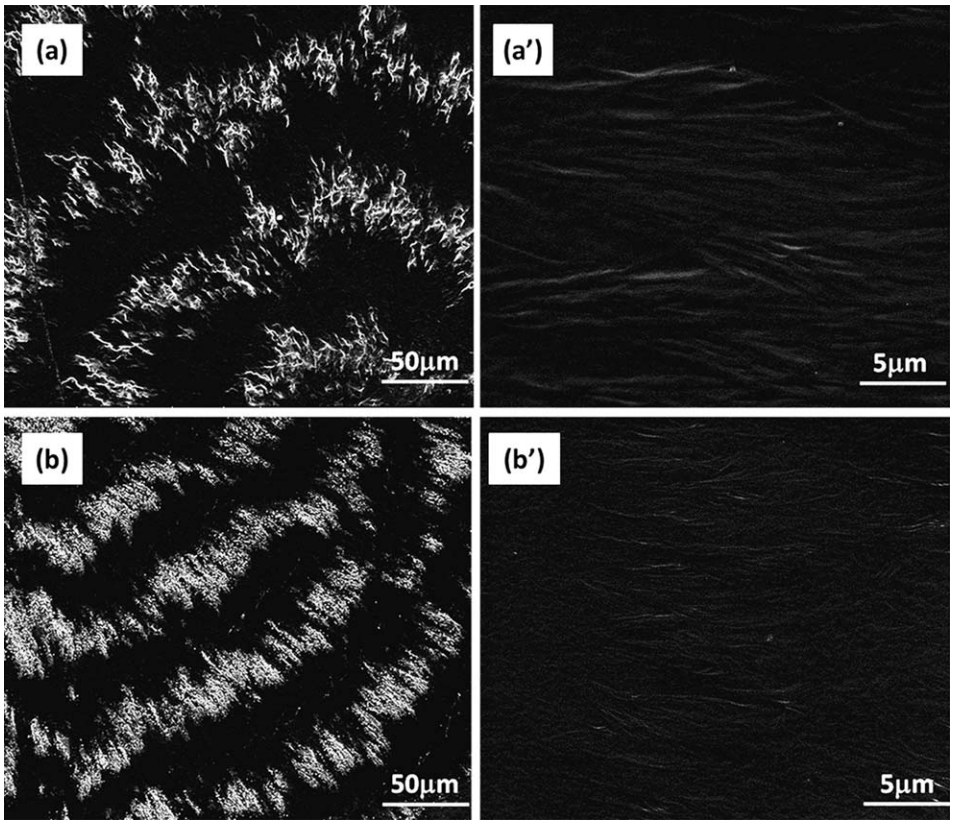

Figure 8. SEM morphology of ring-banded spherulites in PCL/SAN-30 (80/20/) blends with 1 wt % loadings of (a) R974 and (b) A200; a', b' are the magnified micrograph of a, b, respectively.

growth of extinction rings in the blends of PCL/SAN-30/A200 shown in Figure 7 is consistent with that of PCL/SAN-30/R974 blends. Compared with pure PCL/SAN-30 blends, the nucleation density obviously increases with increasing nanosilica content, so that the time for ring-banded spherulites to cover the observed view declines accordingly. Furthermore, ring-banded spherulites in nanosilica filled blends are smaller and variously sized compared with those in pure PCL/SAN-30 blends, especially at higher content. This phenomenon can be attributed to that both homogeneous and heterogeneous nucleation take place in crystallization process, but the rate of homogeneous nucleation is much slower than that of heterogeneous nucleation.[30]

The details of the ring-banded structure are demonstrated by SEM as presented in Figure 8. The bright and dark bands are ridges and valleys under POM, respectively. The ridges with a length of several dozens of microns in SEM images [Figure 8(a,b)] are composed of objects like spindly tree leaves. It has been speculated that the slender leaves are lamellae bundles, not single layer lamellae.[31] Moreover, the growing direction of lamellae is not always parallel to the direction of diameter of spherulite [Figure 8(a',b')]. As a matter of fact, this kind of deflection has twofold influences on lamellae. One is that it leads to the lamellae twisting and another can cause dislocation.[30] Above all, the lamellar twisting mechanism is in

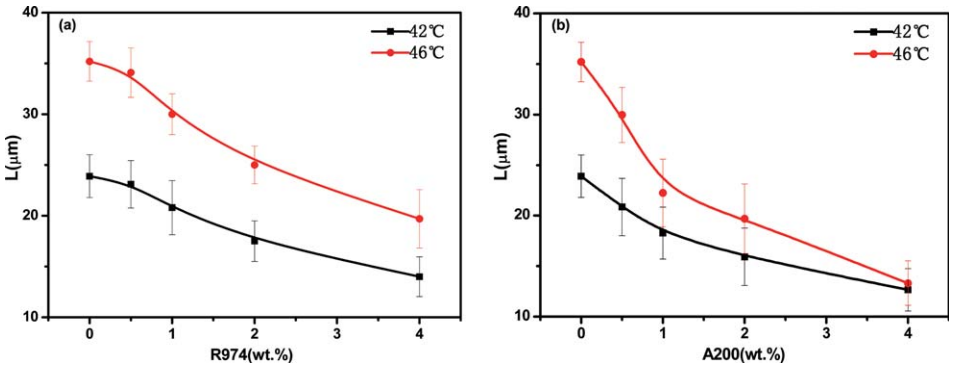

Figure 9. The periodic distance of PCL/SAN-30 (80/20/) blends as a function of nanosilica content with different crystallization temperature, (a) is PCL/SAN/R974 blends, (b) is PCL/SAN/R974 blends. [Color figure can be viewed in the online issue, which is available at wileyonlinelibrary.com.]

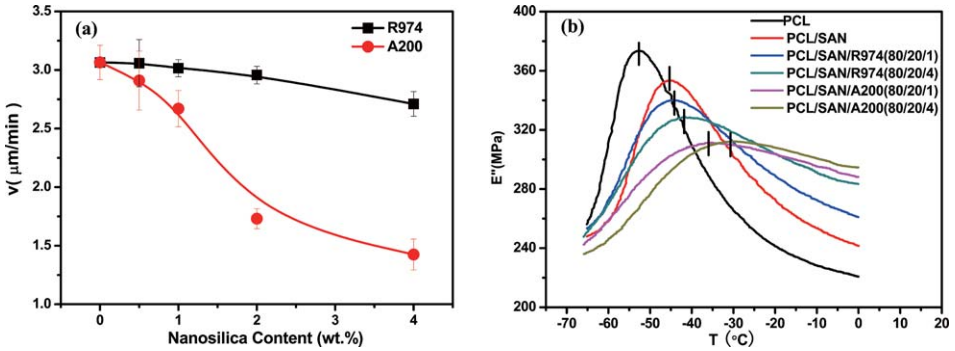

Figure 10. (a) The spherulite growth rate of PCL/SAN-30 (80/20/) blends crystallized at 42 °C and (b) the glass transition temperature as a function of nanosilica content. [Color figure can be viewed in the online issue, which is available at wileyonlinelibrary.com.]

agreement with previous studies to illuminate the formation of ring-banded spherulite in our nanosilica filled blends.[31,32]

Although the pattern and formation mechanism of extinction rings remain unchanged, the average periodicity of extinction rings d (the distance between the two bright rings in Figures 6 and 7) has a downtrend with the increase of the nanosilica content in the blends. Figure 9 shows the composition dependence of the periodic distance, which decreases strongly as the concentration of nanosilica increases from 0 to 4 wt %. In PCL/SAN-30 blends, lamellar twisting frequency is usually revealed by the periodic distance, which is found to diminish at weaker chain mobility in the effect of the improvement of compatibility, according to the half-pitch length of twisted lamellae.[33,34] Kressler *et al.*[7] suggested that greater compatibility would contribute to higher friction coefficient and weaker chain mobility. Combining with the previous analysis, it can be presumed that amorphous components (SAN) have feeblish chain mobility in the front of advancing spherulitic when blends loading with a higher content of nanosilica. Hence, SAN chain segments can hardly spread outside and tend to stay in the inter-lamellar areas, facilitating the twist of lamella throughout the crystallization process.[34] Meanwhile the periodic distance in both kinds of nanosilica filled blends increases with rising crystallization temperature, as has been reported in other polymer blends with ring-banded features.[35,36] Nevertheless, A200 reduce the dependence of the periodic distance on the crystallization temperature more obviously than R974. In PCL/SAN-30/A200 blends, when loading with 4 wt % A200, there is little difference in periodic distance between 42 and 46 °C. It can be attributed to two aspects: (i) for better morphological refinement effect with hydrophilic nanosilica, the periodic distance decreases more sharply with increasing nanosilica content, far greater than the temperature's effect; (ii) the impingements of neighboring spherulites, and a network formed between interactive A200 nanoparticles at higher content shows a weaker sensitivity to temperature compared to that of R974.

Isothermal Crystallization Process of PCL/SAN/Nanosilica Blends

Figure 10(a) shows the trend of growth rate declines with increasing content of both hydrophobic and hydrophilic nanosilica. However, on the addition of 1 wt % or more A200, the growth rate of PCL/SAN-30/A200 blends is far slower than that of PCL/SAN-30/R974 blends. It is considered that polymer blends with better compatibility have higher friction coefficient, which would restrain the polymer chain diffusing from amorphous region to the advancing front of crystal growth, causing a smaller crystallization rate.[7] T_g is generally used to evaluate the mobility of polymer chain segment. Figure 10(b) reveals the T_g of PCL/SAN-30 blends with different content of nanosilica obtained by DMA. It can been seen that the T_g increases with increasing content of nanosilica, and the higher T_g in PCL/SAN/A200 blends indicates weaker chain mobility. In other words, a relative better compatibility between components in the blends has a certain correspondence with the weaker chain mobility of PCL, leading to the reduction of spherulite growth rate.

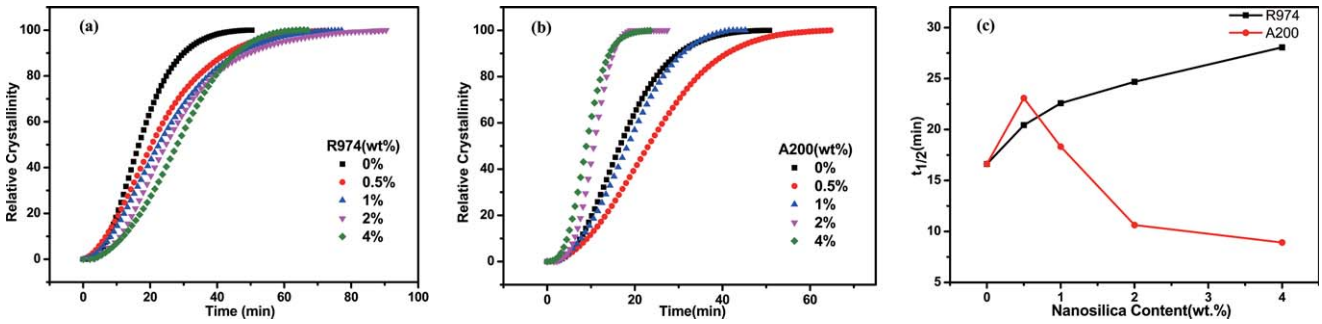

Figure 11. (a,b) Development of relative crystalline of PCL/SAN-30/Nanosilica (80/20/*X*) blends with crystallization time during isothermal crystallization and (c) plots of crystallization half time vs. nanosilica content at 42 °C. [Color figure can be viewed in the online issue, which is available at wileyonlinelibrary.com.]

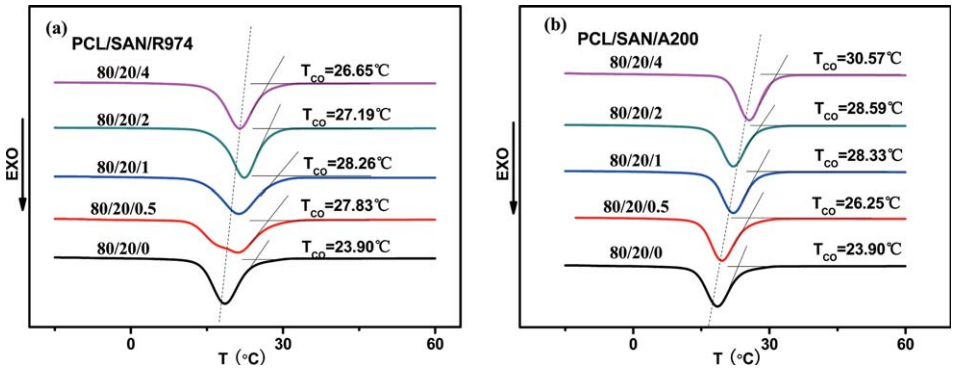

Figure 12. Crystallization curves of PCL/SAN-30 (80/20/) blends filled with nanosilica as measured by DSC. [Color figure can be viewed in the online issue, which is available at wileyonlinelibrary.com.]

In PCL/SAN-30/Nanosilica blends, the evolution of the relative crystallinity vs. time is displayed in Figure 11(a,b). There is a significant dependence of the relative crystalline on the nanosilica concentration. In the investigated content range, the crystallization half-time $t_{1/2}$ of all blends filled with R974 increases with increasing content, while $t_{1/2}$ increases at low content, and then declines as nanosilica content increasing in PCL/SAN-30/A200 blends as shown in Figure 11(c). It suggests that the presence of R974 or low content of A200 ($\leq$1 wt %) impede the crystallization process but A200 with higher content (>1 wt %) facilitate it. A possible explanation for above phenomenon is that, the crystallization kinetic is attached to two factors. One is nucleation rate and another is crystal growth rate. In PCL/SAN-30/R974 blends, the reduction of growth rate caused by R974 plays a dominant role in the investigated range, as well as in low content of A200 ($\leq$1 wt %) filled blends. Once the content of A200 raise up to 2 wt %, the nucleation rate of blends dominate the crystallization kinetic. Di *et al.*[37] also found the isothermal crystallization behavior of PCL/Nanoclay composites was associated with clay concentrations.

Figure 12(a,b) shows the crystallization curves of PCL/SAN-30/Nanosilica blends at a cooling rate of 10 °C/min. In contrast to pure PCL/SAN-30 blends, the crystallization onset temperature (T_{co}) and crystallization peak temperature (T_{cp}) manifest an increase with the incorporation of both types of nanosilica. indicating that nanosilica can lead to the crystallization occurring at higher temperature.[12] What's more, the ability to act as nucleating agent for PCL is limited for the hydrophobic nanosilica and the hydrophilic nanosilica are more effective relatively. That maybe because the hydrogen-bond formed between the silanol group on the surface of hydrophilic nanosilica and the carbanyl group of PCL, can facilitate heterogeneous nucleation.[38] On the whole, the effect of nanosilica on the crystallization behavior of polymer is twofold: nanoparticles provide heterogeneous nucleation sites for crystallization and meanwhile, restrict the growth of crystals.[10,12,37,38] The heterogeneous nucleation effect of high content of A200 (>1 wt %) should dominate over growth restriction effect on the crystallization behavior. On the contrary, the blends loading with R974 or low content of A200 ($\leq$1 wt %) are more likely to exhibit restriction effect rather than nucleation effect.

CONCLUSIONS

The effects of two types of fumed nanosilica (hydrophilic and hydrophobic) on the morphology and crystallization behavior of PCL/SAN-30 blends are investigated. First of all, nanosilica-filled PCL/SAN-30 blends display different refinements effect on morphology depending on the surface nature and concentration of nanosilica. Hydrophilic nanosilica dispersing both at the interface and within the PCL phase lead to a physical compatibilization for the blends, thus compensating the increase of the viscosity ratio, which resulting in a tinier co-continuous morphology, while the hydrophobic nanosilica locating within the PCL phase are less effective. Second, ring-banded spherulites in PCL/SAN-30 blends are observed in the presence of both kinds of nanosilica. Typically, the periodic distance of ring-banded spherulites declines with nanosilica content increasing, which is found to be more apparent for hydrophilic nanosilica filled PCL/SAN-30 blends than that of hydrophobic nanosilica filled blends. And hydrophilic nanosilica reduce the crystallization temperature dependence of the periodic distance more significantly than hydrophobic nanosilica. Furthermore, the lamellar twisting mechanism is utilized to explain the formation of ring-banded spherulites in PCL/SAN blends, which will not be altered by nanosilica. In addition, the crystallization behavior is greatly influenced by the incorporation of nanosilica. In PCL/SAN blends filled with hydrophobic nanosilica, the restriction effect on spherulite growth rate always plays a major role in dominating the crystallization behavior rather than the facilitated heterogeneous nucleation. By contrast, in PCL/SAN blends filled with hydrophilic nanosilica, the crystallization process is associated with the concentration of nanosilica. When blends loading with low content of hydrophilic nanosilica ($\leq$1 wt %), there is more likely to exhibit restriction effect rather than nucleation effect. When blends loading with higher content of hydrophilic nanosilica (>1 wt %), the heterogeneous nucleation effect plays a dominated role in promoting the crystallization behavior, compared to crystal growth restriction effect.

ACKNOWLEDGMENTS

This work is financially supported by State Key Laboratory of Polymer Materials Engineering (Grant No. sklpme2014-2-08) and the National Science of China (51421061).

REFERENCE

1. Chiu, S. C.; Smith, T. *J. Appl. Polym. Sci.* **1984**, *29*, 1797.
2. Wang, Z.; Wang, X.; Yu, D.; Jiang, B. *Polymer* **1997**, *38*, 5897.
3. Ma, D.; Zhang, J.; Wang, M.; Ma, J.; Luo, X. *Macromol. Chem. Phys.* **2001**, *202*, 961.
4. Xu, J.; Guo, B. H.; Zhou, J. J.; Li, L.; Wu, J.; Kowalczuk, M. *Polymer* **2005**, *46*, 9176.
5. Su, C. C.; Lin, J. H. *Colloid. Polym. Sci.* **2004**, *283*, 182.
6. Wang, Z.; Jiang, B. *Macromolecules* **1997**, *30*, 6223.
7. Kressler, J.; Svoboda, P.; Inoue, T. *Polymer* **1993**, *34*, 3225.
8. Martin, G.; Barrès, C.; Sonntag, P.; Garois, N.; Cassagnau, P. *Mater. Chem. Phys.* **2009**, *113*, 889.
9. Laoutid, F.; Estrada, E.; Michell, R. M.; Bonnaud, L.; Müller, A.; Dubois, P. *Polymer* **2013**, *54*, 3982.
10. Li, P.; Huang, Y.; Kong, M.; Lv, Y.; Luo, Y.; Yang, Q.; Li, G. *Colloid. Polym. Sci.* **2013**, *291*, 1693.
11. Liu, X. Q.; Wang, Y.; Yang, W.; Liu, Z. Y.; Luo, Y.; Xie, B. H.; Yang, M. B. *J. Mater. Sci.* **2012**, *47*, 4620.
12. Mdletshe, T. S.; Mishra, S. B.; Mishra, A. K. *J. Appl. Polym. Sci.* **2015**, *132*, DOI: 10.1002/app.42145.
13. He, Y.; Huang, Y.; Li, Q.; Mei, Y.; Kong, M.; Yang, Q. *Colloid. Polym. Sci.* **2012**, *290*, 997.
14. Liu, Y.; Zhao, Z.; Tang, D.; Kong, M.; Yang, Q.; Huang, Y.; Liao, X.; Niu, Y. *Polym. Compos.*, to appear.
15. Lu, X.; Isacsson, U.; Ekblad, J. *Mater. Struct.* **2003**, *36*, 652.
16. Lee, S. H.; Bailly, M.; Kontopoulou, M. *Macromol. Mater. Eng.* **2012**, *297*, 95.
17. Gubbels, F.; Blacher, S.; Vanlathem, E.; Jérôme, R.; Deltour, R.; Brouers, F.; Teyssie, P. *Macromolecules* **1995**, *28*, 1559.
18. Steinmann, S.; Gronski, W.; Friedrich, C. *Polymer* **2002**, *43*, 4467.
19. Li, W.; Karger-Kocsis, J.; Schlarb, A. K. *Macromol. Mater. Eng.* **2009**, *294*, 582.
20. Xia, T.; Huang, Y.; Jiang, X.; Lv, Y.; Yang, Q.; Li, G. *Macromolecules* **2013**, *46*, 8323.
21. Sumita, M.; Sakata, K.; Asai, S.; Miyasaka, K.; Nakagawa, H. *Polym. Bull.* **1991**, *25*, 265.
22. Owens, D. K.; Wendt, R. *J. Appl. Polym. Sci.* **1969**, *13*, 1741.
23. Guggenheim, E. A. *J. Chem. Phys.* **1945**, *13*, 253.
24. Wu, D.; Lin, D.; Zhang, J.; Zhou, W.; Zhang, M.; Zhang, Y.; Wang, D.; Lin, B. *Asian J. Plant Sci.* **2011**, *212*, 613.
25. Elias, L.; Fenouillot, F.; Majesté, J. C.; Cassagnau, P. *Polymer* **2007**, *48*, 6029.
26. Vermant, J.; Cioccolo, G.; Nair, K. G.; Moldenaers, P. *Rheol. Acta* **2004**, *43*, 529.
27. Svoboda, P.; Svobodova, D.; Chiba, T.; Inoue, T. *Eur. Polym. J.* **2008**, *44*, 329.
28. Madbouly, S. A.; Ougizawa, T. *Macromol. Chem. Phys.* **2004**, *205*, 1923.
29. Woo, E. M.; Mandal, T. K.; Lee, S. C. *Colloid Polym. Sci.* **2000**, *278*, 1032.
30. Hua, C.; Chen, Z.; Xu, Q.; He, L. *J. Polym. Sci., Part B: Polym. Phys.* **2009**, *47*, 784.
31. Wang, Z.; An, L.; Jiang, W.; Jiang, B.; Wang, X. *J. Polym. Sci., Part B: Polym. Phys.* **1999**, *37*, 2682.
32. Lotz, B.; Cheng, S. Z. *Polymer* **2005**, *46*, 577.
33. Wang, C.; Thomann, R.; Kressler, J.; Thomann, Y.; Crämer, K.; Stühn, B.; Svoboda, P.; Inoue, T. *Acta Polym.* **1997**, *48*, 354.
34. Zhang, Y.; Fang, H.; Wang, Z.; Tang, M.; Wang, Z. *Cryst Eng Comm* **2014**, *16*, 1026.
35. Xiao, Q.; Yan, S.; Rogausch, K.; Petermann, J.; Huang, Y. *J. Appl. Polym. Sci.* **2001**, *80*, 1681.
36. Wang, T.; Wang, H.; Li, H.; Gan, Z.; Yan, S. *Phys. Chem. Chem. Phys.* **2009**, *11*, 1619.
37. Di Maio, E.; Iannace, S.; Sorrentino, L.; Nicolais, L. *Polymer* **2004**, *45*, 8893.
38. Diao, Y.; Myerson, A. S.; Hatton, T. A.; Trout, B. L. *Langmuir* **2011**, *27*, 5324.